Reducing bubbles in friction lap welded joint of magnesium alloy and polyamide

F. C. Liu*[1], K. Nakata[1], J. Liao[2], S. Hirota[2] and H. Fukui[2]

The direct joining between AZ31B Mg alloy and MC Nylon 6 using friction lap welding (FLW) was performed over a wide range of welding parameters to clarify the effect of welding parameters on bubble formation for the purpose of obtaining high strength hybrid joints without bubbles. The volume of bubbles in the FLW joints was influenced by the amount of gases generated due to the pyrolysis of Nylon 6 and the amount of gases squeezed out of the joints during welding. An appropriate increase in welding speed, tool rotation rate and plunge depth can reduce the volume of bubbles. Strong FLW joint with area fraction of bubbles <8% was obtained after welding process optimisation.

Keywords: Friction lap welding, Joining, Metal, Polymer, Mechanical property, Thermal degradation

Introduction

Recently, increasing interest has been focused on the application of polymers, polymeric composites and light alloys to fabricate industrial components due to the weight saving considerations and the current emission reduction policies.[1] Nowadays, polymeric materials exhibit not only improved mechanical performance but also highly insulated and corrosion resistance along with increased design freedom to manufacture products.[2] Light weight alloys have become more mechanically reliable and also cheaper owing to the processing and fabrication advance supported by the fast development in industry fields.[3,4]

The joining of plastic and metal is generally performed using adhesive bonding (glues) or mechanical fastening such as bolts and rivets.[1] However, these joining processes have some problems such as long processing time, accidental disassembly and susceptibility to degradation by environmental factors.[1,5,6] Promising techniques for the joining of metal to plastic, such as friction welding,[7,8] friction spot joining,[9–11] laser joining[6,12,13] and ultrasonic welding,[14,15] have arisen to solve these problems. Although these emerging joining techniques offer alternative methods compared to the traditional techniques for the realisation of hybrid metal–plastic joints, these new joining techniques are still in the developmental stage, and more studies still need to promote the application of these techniques.

Friction lap welding (FLW) of a metal to a polymer, which was developed in Joining and Welding Research Institute, Osaka University, is a new conception of joining method for metal–plastic hybrid joints.[7] The basic conception of FLW is simple: a non-consumable rotation tool is pressed on the surface of metal matrix and travels long the overlap region. The main difference between the FLW and FSW is that the FLW tool does not have a stir pin,[16,17] and therefore, the primary function of the rotation tool is to press and heat up the metal workpiece. The heat accomplished by friction between the tool shoulder and the metal workpiece transfers via conduction from the metal component to the plastic component and consequently melts the plastic materials in a narrow region beside the interface. Bonding between the metal and the plastic can be finished after the melted plastic is solidified under the pressure provided by the pressed metal component. Friction lap welding can be performed using the existing friction stir welding (FSW) machines or modified machine tools. This enhances the design flexibility of FLW and makes the FLW process suitable for automation and robot use.

The effective of FLW for joining metal and plastic has been demonstrated through a case study on 6061 Al alloy and MC Nylon 6.[8] The lap joints with high shear strength were obtained over a wide range of welding parameters. The welding temperatures were estimated higher than 400°C,[16,18] and the MC Nylon 6 will be pyrolysed at temperatures higher than 350°C.[19] Therefore, a number of bubbles will be generated in the nylon because parts of the Nylon 6 near the joint interface were pyrolysed at the high welding temperatures. Similar bubbles were also extensively observed in the hybrid joints of metal and plastic fabricated by other welding techniques.[10,12,14] These bubbles have no load bearing ability and increase the stress concentration under cyclic loading. The hybrid joints containing high levels of bubbles will not be accepted according to Japanese Industrial Standards. Therefore, it is necessary to understand the bubble generation and its influence factors during FLW and then endeavour to reduce the volume of bubbles in the joints.

[1]JWRI, Osaka University, 11-1 Mihigaoka Ibaraki, Osaka 567-0047, Japan
[2]Kurimoto Ltd, 2-8-45 Suminoe, Osaka 559-0021, Japan

*Corresponding author, email fchliu@alum.imr.ac.cn

F. C. Liu is an 'international research fellow of the Japan Society for the Promotion of Science'.

Published by Maney on behalf of the Institute
Received 3 April 2014; accepted 19 June 2014
DOI 10.1179/1362171814Y.0000000228

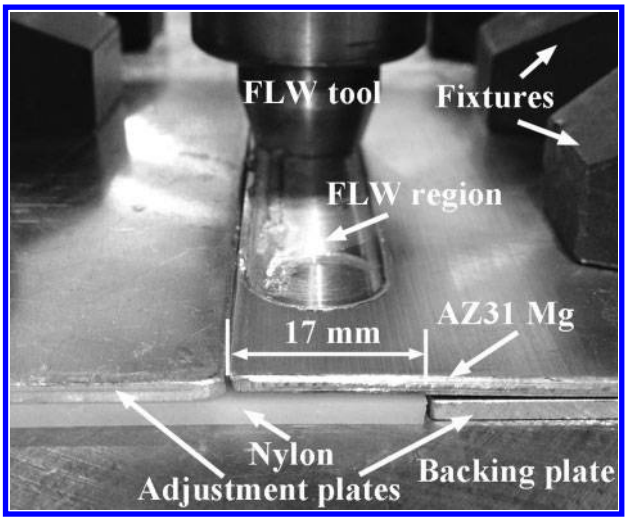

1 Workpiece set-up for FLW using cylindrical tool with dimension of 15 mm in root diameter (width of overlap region is 17 mm)

In this study, the direct lap joining between two commercially available materials AZ31B Mg alloy and MC Nylon 6 was performed using FLW over wide welding parameters. Compared with normal Nylon 6, MC Nylon 6 has the advantages of a simple preparation procedure, high crystallinity, high molecular weight and excellent properties. The main purpose is to provide a deep understanding about the influence of FLW parameters on the bubbles and the joining strength and therefore obtain high strength FLW joints with a low volume of bubbles to meet the requirement of practical industries.

Experimental

AZ31B Mg alloy and MC Nylon 6 plates with dimensions of $150 \times 75 \times 2$ mm were used for FLW experiments. The chemical composition of the AZ31B Mg alloy is Mg–3·34Al–1·13Zn–0·35Mn–0·02Si–0·001Cu–0·002Fe–0·0001Ni (wt-%). The MC Nylon 6 was prepared by the alkali catalysed anionic ring opening polymerisation of caprolactam. The physical properties of the MC Nylon 6 has been summarised in our previous study.[8] In order to investigate the influence of FLW parameters on the shear strengths of the lap joints, a small overlap width should be selected for the purpose of making the FLW joints fail through the welding interface and therefore working out the shear strengths. For this reason, an overlap of 17 mm was used to join the AZ31B Mg alloy and MC Nylon 6. The surface of AZ31B plates were mechanically ground using 800-grit sand papers before FLW. Friction lap welding was conducted under a position control system using a cylindrical tool with dimension of 15 mm in root diameter. The workpiece set-up is shown in Fig. 1. The cylindrical tool remained perpendicular to the workpiece surface for all the FLW process. The FLW parameters and the sample designation are summarised in Table 1.

The cross-sections for joint interface examinations were mechanically ground and polished with 1 μm diamond paste and then subjected to optical microscopy (OM) and scanning electron microscopy–secondary electron imaging (SEM-SEI) examination. In order to reveal the grain structures of the AZ31B Mg alloys, the samples were etched with an etching reagent consisting of 4·2 g picric acid, 10 mL distilled water and 70 mL ethanol before OM examination. Twenty cross-sections for each FLW sample were examined using SEM to estimate the area fraction of bubbles. The length of each bubble L_i along the joining interface can be measured. The area fraction of bubbles f for each cross-section can be obtained using equation (1)

$$f = \frac{\sum L_i}{L_O} \quad (1)$$

where $\sum L_i$ is the total length of all the bubbles on the cross-section, and L_O is the length of welding interface observed on the cross-section. Ten hardness points were measured in the middle of the cross-sectional weld region for each sample using a Vickers hardness tester with a load of 300 g for 13 s.

The FLW samples were cut into strips ~20 mm in width perpendicular to the welding direction for tensile shear test. Tensile shear test was carried out using a tensile test machine (SHIMAZU) at a tensile speed of 0·5 mm min^{-1}. The grip inserts were used so that the centreline of the grip assembly was aligned with the joint interface. The fracture surfaces of the tensile samples were subjected to analyses by OM and SEM and energy dispersive X-ray spectrometer equipped with SEM (SEM-EDS).

Results and discussion

Load bearing ability of FLW joints

The tensile shear test results of FLW joints produced using well designed parameters M1 to M8 are given in Fig. 2. Figure 2*a* shows that an increase in the welding speed from 200 to 800 mm min^{-1} reduced slightly the tensile shear strength failure load (TSSFL) of the joints

Table 1 Welding parameters and sample designations for FLW joints of AZ31B/MC Nylon 6

Sample designation	Shoulder diameter/mm	Plunge depth/mm	Rotation rate/rev min^{-1}	Welding speed/mm min^{-1}
M1	15	0·27	2000	200
M2	15	0·27	2000	400
M3	15	0·27	2000	800
M4	15	0·27	2000	1500
M5	15	0·27	1000	800
M6	15	0·27	3000	800
M7	15	0·17	2000	800
M8	15	0·54	2000	800
M9	15	0·27	4000	1500
M10	15	0·54	4000	1500
M11	15	0·81	4000	1500

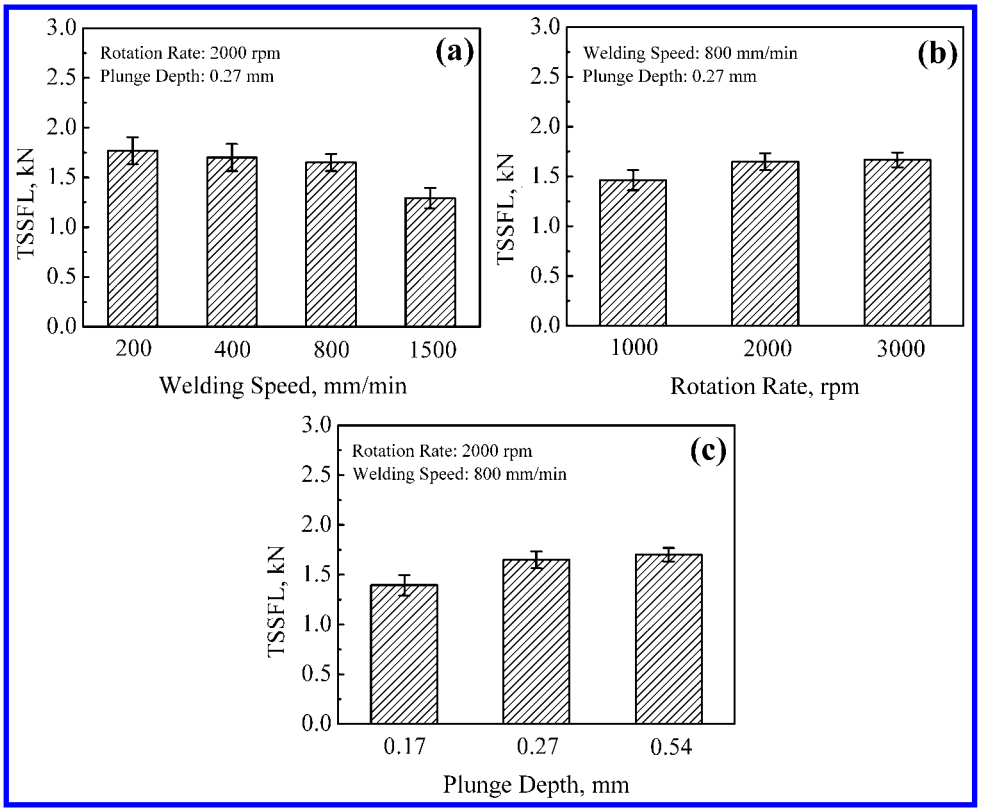

2 Tensile shear properties of FLW joints produced at different *a* welding speed, *b* tool rotation rate and *c* tool plunge depth

from 1·75 to 1·65 kN and obviously reduced the TSSFL to 1·29 kN at 1500 mm min^{-1}. In industry operation, it is usually expected to conduct the welding process at higher welding speed for productivity. Therefore, FLW was conducted at 800 mm min^{-1} to identify the influences of rotation rate and plunge depth on FLW joints. It was observed that an increase in the rotation rate from 1000 to 3000 rev min^{-1} increased the TSSFL from 1·46 to 1·70 kN (Fig. 2*b*). Similarly, an increase in the plunge depth from 0·17 to 0·54 mm led to an increase in the TSSFL from 1·39 to 1·70 kN (Fig. 2*c*).

Cross-section examination of FLW joints

Figure 3 shows the cross-sections of the FLW joints produced using parameters M1 to M8. A number of bubbles were clearly observed inside the resolidified layer of nylon. A magnified image shows that the bubble did not contact the AZ31B plate directly but was separated from the AZ31B by a thin nylon film. The bubble regions extended to around 30–300 μm inside the nylon depends on the welding parameters. Similar bubble morphology was also observed in FLW joints of MC Nylon 6 and 6061 Al.[8] The bubble region in the lap joint between AZ91D Mg alloy and polyethylene terephthalate produced by laser beam also extended to ~175 μm in a narrow region before the interface.[6]

During FLW, the MC Nylon 6 beside the AZ31B plate was melted, resulting in a lack of supporting force from the MC Nylon 6 to the AZ31B plates. Therefore, the AZ31B plates bowed into the melted nylon in the FLW region under the down force of FLW tool. The melted nylon was resolidified after FLW and could be clearly observed on the cross-sections of the FLW joints. Because the AZ31B plates were pushed toward the melted nylon during FLW, part of melted nylons were squeezed out of the joints. For this reason, the thickness of melted nylon was not measured directly from the cross-sections of the hybrid joints, but was calculated as the difference between the initial thickness of nylon plate and the thickness of unmelted nylon. The initial thickness of nylon plate was 2 mm. The thickness of unmelted nylon could be measured directly on the cross-sections of the hybrid joints.

The variation in thickness of melted nylon with welding parameters was summarised in Fig. 4*a*. The thickness of melted nylon increased with an increase in the rotation rate or a decrease in the welding speed. This trend is in good agreement with the investigation on FLW of AA 6061Al and MC Nylon 6.[8] It is also noted that an increase in the plunge depth also increased the thickness of melted nylon.

The variation in thickness of melted nylon (H) with $(R/v)^{0·5}$ for FLW joints welded at the plunge depth of 0·27 mm is plotted in Fig. 4*b*. R (rev min^{-1}) is the rotation rate, and v (mm min^{-1}) is the welding speed. For comparison, a line predicted by equation (1), which was used to express the relationship of H and $(R/v)^{0·5}$ for FLW joints of AA 6061 and MC Nylon 6 was also included. It is found that a linear relationship exists between H and $(R/v)^{0·5}$, and the data from FLW joints of AZ31B Mg and MC Nylon 6 fit well with equation (2)

$$H = 0{\cdot}25\left(\frac{R}{v}\right)^{0·5} \tag{2}$$

Figure 5 shows the cross-sectional micrograph of the AZ31B basal materials (BMs) and AZ31B alloys in the middle of the weld region for sample M1. The BM

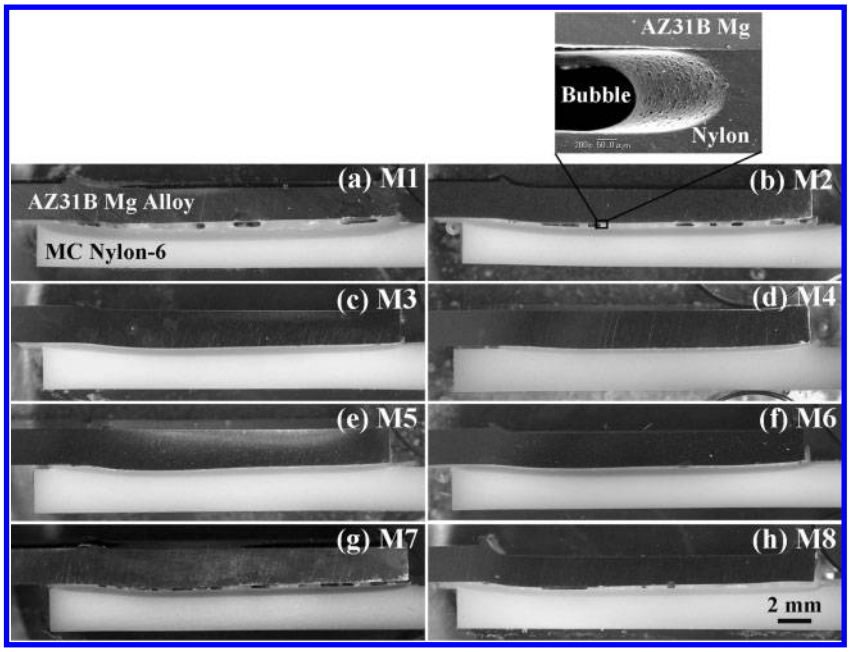

3 Cross-sectional macrograph of FLW joints produced using different FLW parameters M1 to M8

shows inhomogeneous grains, which are the typical rolled microstructure of the magnesium alloys. The average grain size of the BM was determined to be ~12·5 μm. As typically shown in Fig. 5*b*, the AZ31B Mg alloys in the weld region experienced high temperature thermal cycles, resulting in an obvious and homogeneous grain growth.

The influence of welding parameters on the grain growth and hardness values in the weld region is summarised in Fig. 6. All the average grain sizes of AZ31B Mg alloy in the weld region were higher than of BM. With a decrease in the welding speed from 1500 to 200 mm min^{-1}, the average grain size increased from 16·9 to 23·9 μm due to the increased thermal input. Similarly, with an increase in the rotation rate from 1000 to 3000 rev min^{-1} and in the plunge depth from 0·17 to 0·54 mm, the average grain size increased from 17·1 to 20·6 μm and from 17·6 to 21·2 μm respectively.

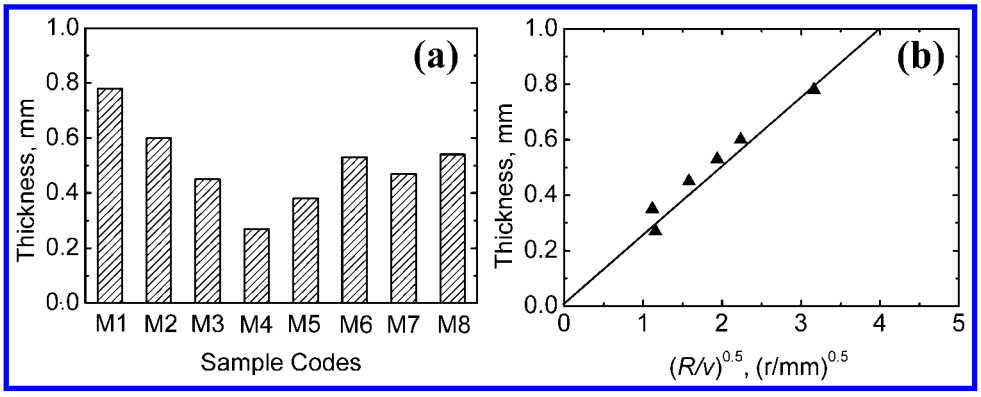

4 Variation in thickness of melted nylon with *a* welding parameters and *b* $(R/v)^{0·5}$

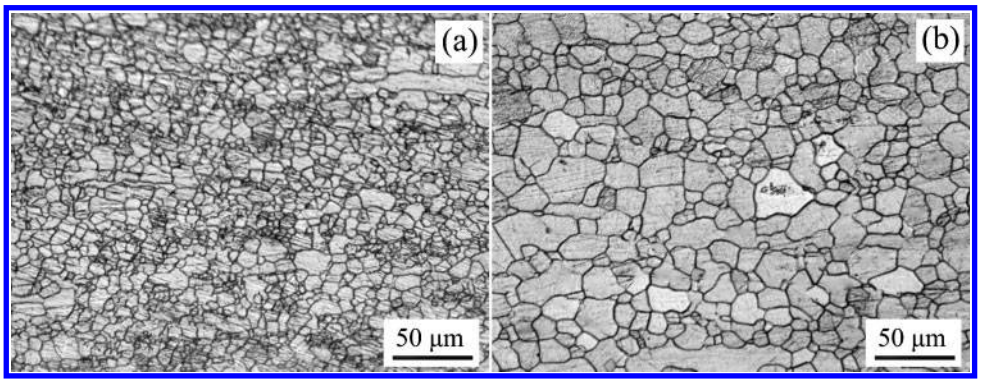

a base materials; *b* weld region of sample M1

5 Microstructure of AZ31B Mg alloy

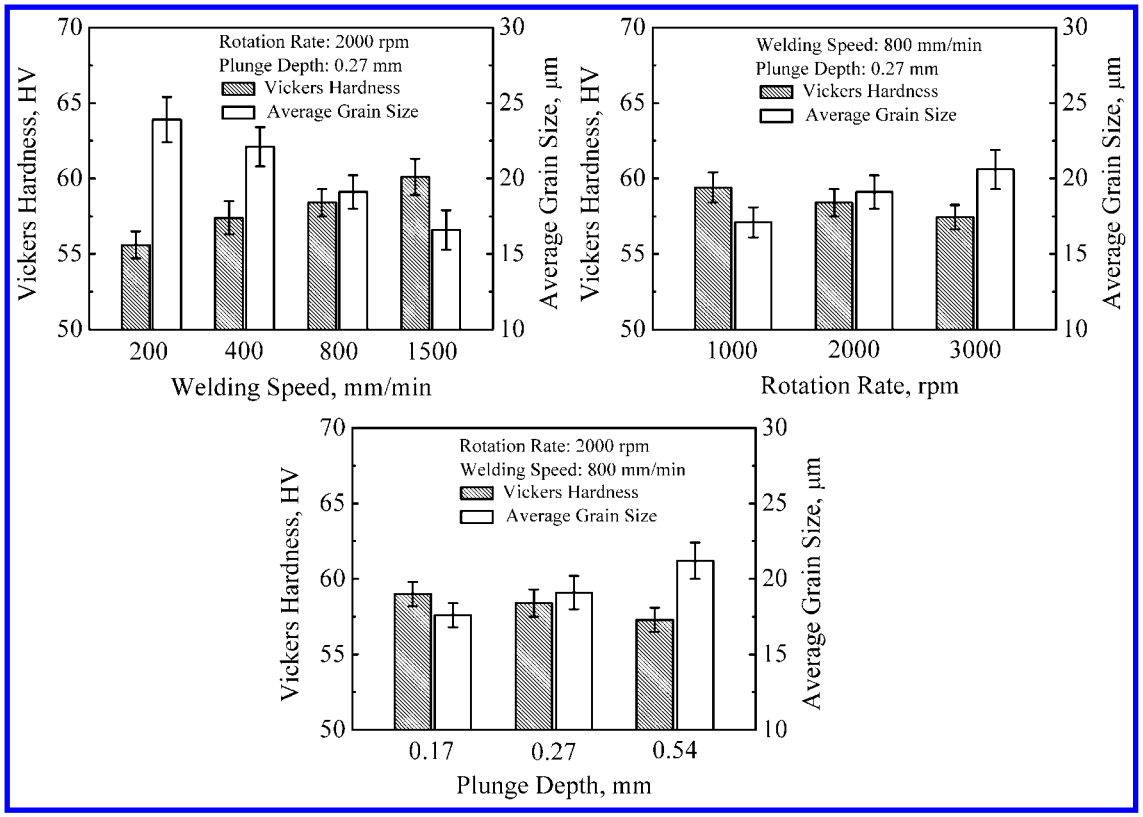

6 Variation in Vickers hardness and average grain size with *a* welding speed, *b* rotation rate and *c* plunge depth

According to the Hall–Petch relationship in the friction-stir-welded AZ31B Mg alloy, the finer grain structure would result in a higher value of hardness in the SZ as compared to the thermal mechanical affected zone and heat affected zone.[20] Since the grain boundaries were the main obstacle to the slip of dislocations, the materials with a larger grain size would have a weaker resistance to the localised plastic deformation due to the presence of less grain boundaries, giving rise to a lower hardness. The present study also showed that the larger grain size of AZ31B Mg alloys in the weld region led to a lower average hardness value for all the FLW joints.

Influence of FLW parameters on bubble formation

In order to observe the bubbles in the FLW joints in detail, the fracture surfaces of the FLW joints were subjected to optical examinations. As shown in Fig. 7, residual nylons were detected as light areas on the fracture surfaces of all the AZ31B plates. The distribution of residual nylon on AZ31B plates was highly dependent on the welding parameters. It was found that the melted nylon region for the sample processed at 1500 mm min^{-1} was narrower than the overlap region due to the low thermal input (Fig. 7*d*). This may partly respond to the low strength of the FLW joint produced at 1500 mm min^{-1} (Fig. 2*a*).

In order to reveal the morphological details, the fracture surfaces of the FLW joints were subjected to metal spraying and then SEM-SEI and SEM-EDS examinations. The SEM-EDS examination showed that no Mg alloy was embedded in the nylon part of the fracture surfaces, indicating that the joints did not failed in the Mg alloy. Examinations by SEM-SEI were conducted on the fracture surfaces of the AZ31B Mg alloy for sample M1 as a typical example in Fig. 8*a*. Three different regions I–III were distinguished by a black, a grey and a white region respectively. Figure 8*b* shows the carbon distribution of Fig. 8*a* using SEM-EDS map. Carbon was detected in regions I and II, which means that the residual nylon existed in these regions. High magnification observation shows that region I was characterised by spherulitic morphology as shown in Fig. 8*c*. Similar spherulites were also observed on the directly opposite MC Nylon 6. These demonstrated that the nylons detected in region I were the nylon films attached on the AZ31B plate in the bubble regions (Fig. 3). That is to say, region I correspond to the bubbles in the FLW joints.

High magnification SEM observation in Fig. 8*d* and carbon distribution in Fig. 8*e* showed that region II was covered by high density of fractured nylons, demonstrating the occurrence of cohesive fracture in the nylon. A few nylon particles also existed in region III as shown in Fig. 8*f* and *g* , though they were hard to be observed through optical examination (Fig. 7*a*). The scratches made by mechanically grinding the Mg plate were clearly visible in region III, but were hard to be observed in region II because the scratches were almost totally covered by nylons. It is estimated that region II has a higher TSSFL contribution than region III because thicker residual nylon were observed in region II. It is noted that the density of carbon along the scratches was higher than that between the scratches, indicating that more residual nylons were left in the scratches. This should be partly attributed to the enlarged joining area in the scratches. It can be deduced that the strength of the FLW joints can be improved by increasing the surface roughness of AZ31B plates.

Figure 9 shows the morphology of bubbles observed on fracture surface of the joints made by parameters M2

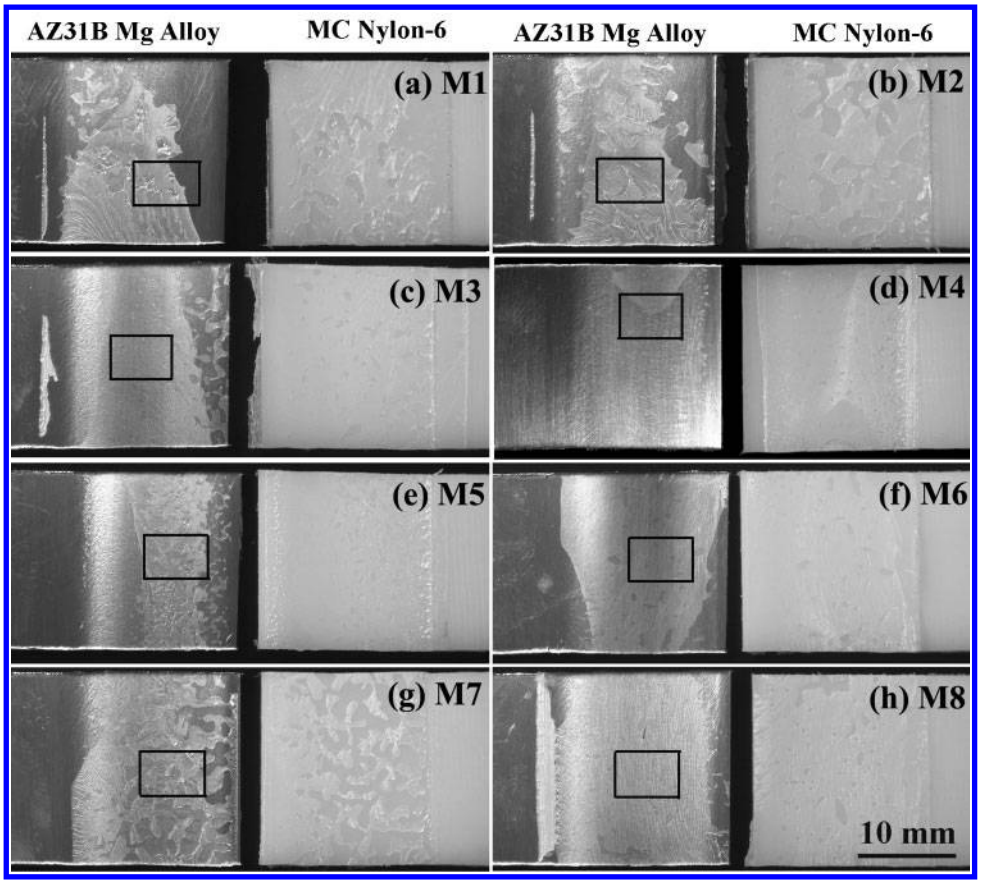

7 Comparing fracture surface of FLW joints after tensile shear test by OM observation for different FLW parameters M1 to M8 respectively (left is AZ31B Mg alloy side and right is MC Nylon 6 side in each photo)

to M8. The size of bubbles was significantly reduced with increasing the welding speed from 400 to 1500 mm min^{-1} as shown in Fig. 9*a–c*. When increasing the rotation rate from 1000 to 3000 rev min^{-1} (Fig. 9*b, d* and *e*) or increasing the plunge depth from 0·17 to 0·54 mm (Fig. 9*b, f* and *g*), the morphology of bubbles was changed from the large irregular shaped and interconnected ones to independent small circular ones.

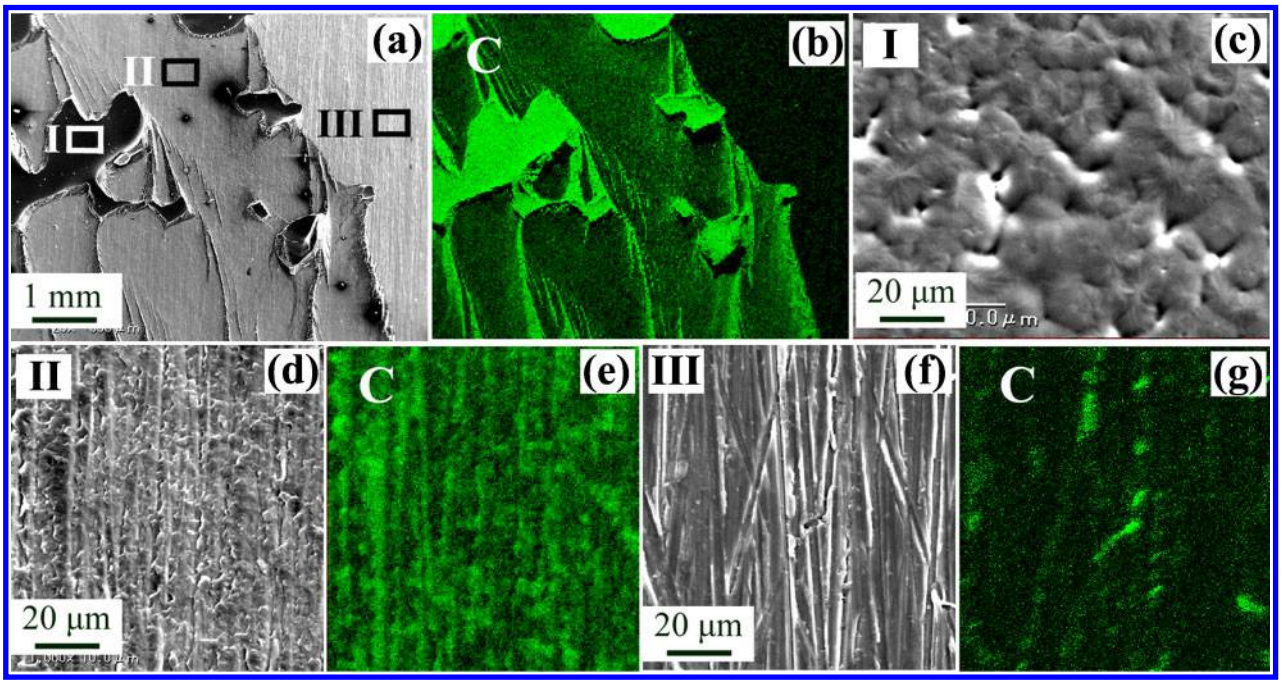

a low magnify SEI map; *b* carbon distribution in *a*; *c*, *d* and *f* high magnification SEI image of region I, II and III respectively; *e*, *g* carbon distribution of region II and III respectively

8 Typical SEM-SEI and EDS carbon distribution on fracture surface of AZ31B Mg alloy side for sample M1 (inspected region was indicated by black box in Fig. 4*a*)

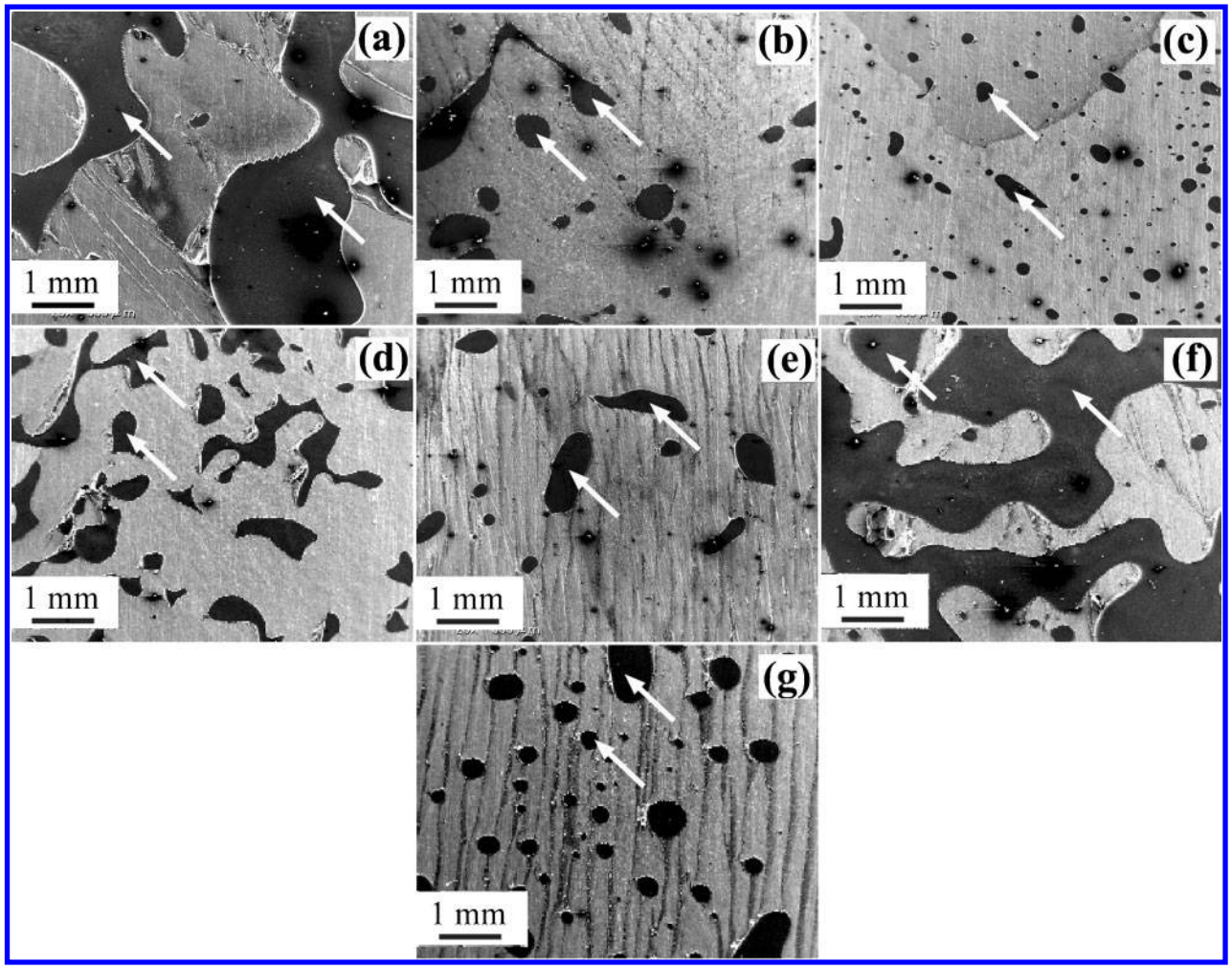

a M2; *b* M3; *c* M4; *d* M5; *e* M6; *f* M7; *g* M8

9 Images (SEM) of bubble morphology on fracture surface of AZ31B Mg alloy side for samples in rectangular region illustrated in Fig 4 (bubbles corresponded to black coloured regions in each SEI image as typically bubbles indicated by arrows)

The influence of FLW parameters on the area fraction of bubbles is given in Fig. 10. The area fraction of bubbles in the FLW joints decreased with the increase in welding speed, rotation rate and/or plunge depth.

It is suggested that the formation of bubbles in the FLW joints is attributed to the thermal degradation of plastics.[8,12] The thermal degradation of Nylon 6 has been studied by pyrolysis gas chromatography.[19] The cumulative degradation products reached 8×10^5 units after the pyrolysis was performed in the gas chromatography flame ionisation detection equipment at 350°C for ~3000 s. When the pyrolysis was performed at 400, 450 and 500°C, 10×10^5 units of pyrolysis products were obtained within 150, 10 and 4 s respectively. That is to say, an increase in either peak temperature or high temperature duration during the FLW resulted in higher volume of pyrolysis gases.

The influence of welding parameters on thermal input for FLW and FSW is similar because the peak temperature and high temperature duration in the friction stir welded joints made with and without pin were close to each other.[16,17,21] An increasing in the tool rotation rate might increase the peak temperature slightly, but did not change the high temperature duration remarkably. In contrast, a decrease in the welding speed could increase both the peak temperature and high temperature duration. It was reported that the peak temperature at the back of the FSW AZ31B plates with a thickness of 4 mm was ~450°C.[18] In the present work, the thickness of AZ31B plates was 2 mm, so that the peak temperature at the back surface of the AZ31B plates of FLW joints could be slightly higher. For this reason, Nylon 6 was pyrolysed, and bubbles were formed in the FLW joints.

The area fraction of bubbles in the FLW joints was influenced by the amount of gases generated due to the pyrolysis of Nylon 6 and the amount of gases squeezed out of the joints during FLW. The ejection of pyrolysis gases out of the joints was due to the fact that the AZ31B plate was bowed toward the MC Nylon 6 plate when the rotated FLW tool was passing through the welding region. This can be verified by the cross-sectional observation of the FLW joints (Fig. 3), in which the Mg plates were curved toward the nylon side. If the AZ31B plate was heavily bowed toward the nylon plates during FLW, a large volume of melted nylon and pyrolysis gases would be squeezed out of the FLW joints.

As the welding speed was reduced, the amount of gases generated due to the pyrolysis of Nylon 6 was greatly increased due to both the elevated peak temperature and extended high temperature duration.

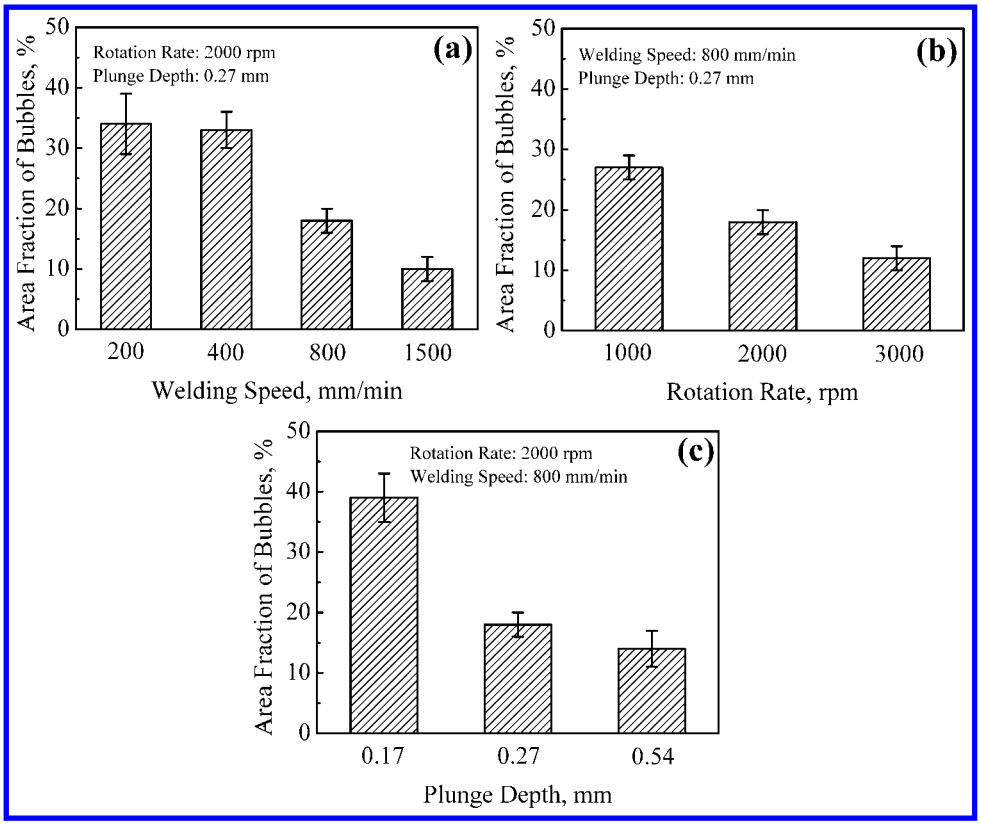

10 Variation in area fraction of bubbles with *a* welding speed, *b* rotation rate and *c* plunge depth

The amount of gases squeezed out of the joints during FLW might also be increased since the AZ31B plates were bowed increasingly toward the MC Nylon 6 plates when the AZ31B plates were further softened due to the increased thermal input. This study shows that the area fraction of bubbles was increased from 10 to 34% with reducing the welding speed from 1500 to 200 mm min^{-1}, indicating that the increase in the amount of gases generated due to increased heat input and temperature and therefore pyrolysis of Nylon 6 was dominant (Fig. 10*a*).

An increase in the tool rotation rate might increase the peak temperature slightly, but did not change the high temperature duration remarkably. Therefore, as the tool rotation rate was increased, the amount of gases generated due to the pyrolysis of Nylon 6 was not greatly increased, but the amount of gases squeezed out of the joints during FLW might be augmented because the AZ31B plates were further softened and the AZ31B plates were bowed increasingly toward the MC Nylon 6 plates. As a result, the area fraction of bubbles was decreased from 27 to 12% with increasing the tool rotation rate from 1000 to 3000 rev min^{-1} (Fig. 10*b*). Similarly, as the plunge depth was increased, the AZ31B plate was also heavily bowed toward the nylon plate during FLW, so that a larger volume of melted nylon and pyrolysis gases were squeezed out of the FLW joints, and thus, the area fraction of bubbles tended to be decreased with increasing the plunge depth (Fig. 10*c*).

Friction lap welding at extremely high welding speed

The results of parametric experiment and analysis indicated that the volume of bubbles can be reduced through increasing either welding speed, tool rotation rate or tool plunge depth. Therefore, FLW was further conducted at a welding speed of 1500 mm min^{-1}, a tool rotation rate of 4000 rev min^{-1}, (which are the maximum welding speed and rotation rate of the present FLW machine) and various plunge depths. Figure 11 shows that with increasing the plunge depth from 0·27 to 0·54 mm, the TSSFL increased from 1·80 to 1·91 kN and the area fraction of bubble decreased from 12 to 8%. In contrast, the TSSFL decreased to 1·84 kN, and the area fraction of bubbles increased to 16% when the plunge depth reached 0·81 mm. It was found that the fracture surface of Mg alloy side was changed into dark black for the sample produced at the plunge depth of 0·81 mm (Fig. 12), indicating a significant increase in welding temperature. This demonstrated that high volume of gas can be generated from the pyrolysis of MC Nylon 6 in a very short time when the welding temperature is fairly high.

Therefore, the adequate increase in the plunge depth is recommended to decrease the bubble formation and to increase the joint strength, but unlimited increase in the plunge depth should be avoided.

Relationship between TSSFL and area fraction of bubbles

Figure 13 shows the variation in TSSFL with area fraction of bubbles. Sample M4 was not included in Fig. 13 because its melted nylon region was much narrower than the overlap region due to the insufficient thermal input (Fig. 7*d*). The data are slightly scattered because the samples produced at low welding speeds, which contains high area fraction of bubbles, also exhibited high TSSFL. This should be attributed to the

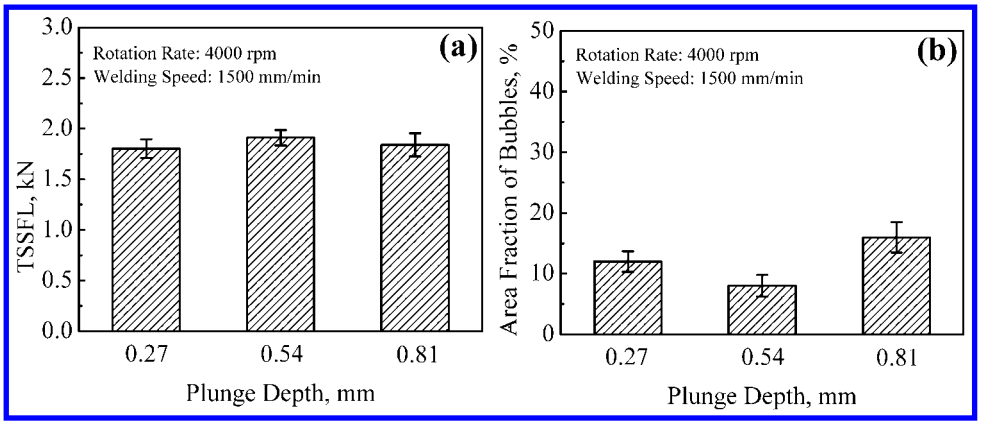

11 Variation in *a* TSSFL and *b* area fraction of bubbles with plunge depth for sample welding at 4000 rev min^{-1} and 1500 mm min^{-1}

fact that the joining strength along the interface was enhanced when the chemical interaction time at high temperature between the Mg alloy and the nylon turned longer. This implies that there is an adhesive bond component between the Mg alloy and MC Nylon 6. Such joints obtained at low welding speed, however, will not be recommended due to their high levels of bubbles. All the samples that contained low area fraction of bubbles exhibited considerable high TSSFL. The bubble regions did not contribute to the shear strength because the FLW joints fractured across the bubbles during the tensile shear test. Therefore, reducing the volume of bubbles is beneficial to the enhancement in the strength of the FLW joints.

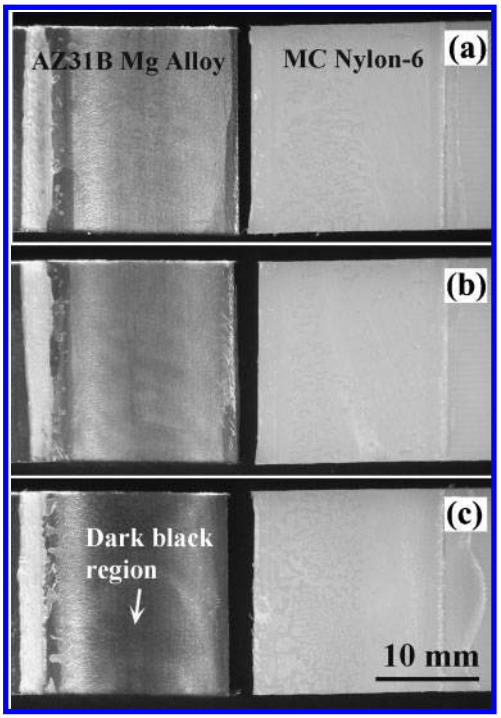

12 Effect of plunge depth on fracture surface after tensile shear test of FLW joints produced with different plunge depths *a* 0·27 mm, *b* 0·54 mm and *c* 0·81 mm at constant rotation rate of 4000 rev min^{-1} and welding speed of 1500 mm min^{-1} for parameters M9, M10 and M11 respectively

Conclusions

Friction lap welding of AZ31B Mg alloy and Nylon 6 was investigated over a wide range of welding parameters to demonstrate the effect of welding parameters on the bubble formation for the purpose of obtaining high strength hybrid joints without bubbles. The main conclusions are as follows.

1. AZ31B magnesium alloy and MC Nylon 6 could be directly joined together using FLW.
2. The volume of bubbles was determined by the amount of gases generated due to the pyrolysis of Nylon 6 and the amount of gases squeezed out of the joints during FLW. An appropriate increase in welding speed, tool rotation rate and tool plunge depth can reduce the volume of bubbles.
3. The strength of the FLW joints was enhanced via reducing the volume of bubbles. A strong FLW joint with a very tiny amount of bubbles was obtained at a welding speed of 1500 mm min^{-1}, a tool rotation rate of 4000 rev min^{-1} and a plunge depth of 0·54 mm.

Acknowledgements

This work was partly supported by Grant-in-Aid for Scientific Research (A) (grant no. 21246111) from Japan Society for Promotion of Science (JSPS). One of the authors (F. C. Liu) wishes to acknowledge the support of FY 2014 JSPS Postdoctoral Fellowship for Foreign Researchers.

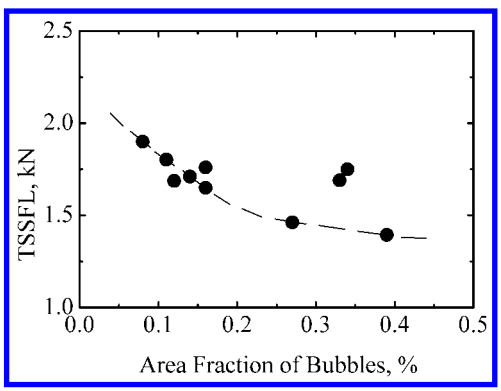

13 Influence of area fraction of bubbles on TSSFL of FLW joints with different parameters

References

1. S. T. Amancio Filho and J. F. dos Santos: 'Joining of polymers and polymers–metal hybrid structures: recent developments and trends', *Polym. Eng. Sci.*, 2009, **49**, 1461–1476.
2. C. Gao, L. Yu, H. Liu and L. Chen: 'Development of self-reinforced polymer composites', *Prog. Polym. Sci.*, 2012, **37**, 767–780.
3. B. L. Mordike and T. Ebert: 'Magnesium: properties–application–potential', *Mater. Sci. Eng. A*, 2001, **A302**, 37–45.
4. W. S. Miller, L. Zhuang, J. Bottema, A. J. Wittebrood, P. De Smet, A. Haszler and A. Vieregge: 'Recent development in aluminium alloys for the automotive industry', *Mater. Sci. Eng. A*, 2000, **A280**, 37–49.
5. A. Fink, P. P. Camanho, J. M. Andres, E. Pfeiffer and A. Obst: 'Hybrid CFRP/titanium bolted joints: performance assessment and application to a spacecraft payload adaptor', *Compos. Sci. Technol.*, 2010, **70**, 305–317.
6. M. Wahba, Y. Kawahito and S. Katayama: 'Laser direct joining of AZ91D thixomolded Mg alloy and amorphous polyethylene terephthalate', *J. Mater. Process. Technol.*, 2011, **211**, 1166–1174.
7. K. Nakata: International Patent Application no. PCT/JP2012/053839.
8. F.C. Liu, J. Liao and K. Nakata: 'Joining of metal to plastic using friction lap welding', *Mater. Des.*, 2014, **54**, 236–244.
9. S. T. Amancio Filho, C. Bueno, J. F. dos Santos, N. Huber and E. Hage, Jr: 'On the feasibility of friction spot joining in magnesium/fiber reinforced polymer composite hybrid structures', *Mater. Sci. Eng. A*, 2011, **A528**, 3841–3848.
10. S. M. Goushegir, J. F. dos Santos and S. T. Amancio Filho: 'Friction spot joining of aluminum AA2024/carbon-fiber reinforced poly (phenylene sulfide) composite single lap joints: microstructure and mechanical performance', *Mater. Des.*, 2014, **47**, 176–206.
11. F. Yusof, Y. Miyashita, N. Seo, Y. Mutoh and R. Moshwan: 'Utilising friction spot joining for dissimilar joint between aluminium alloy (A5052) and polyethylene terephthalate', *Sci. Tech. Weld. Join.*, 2012, **17**, 544–549.
12. S. Katayama and Y. Kawahito: 'Laser direct joining of metal and plastic', *Scr. Mater.*, 2008, **59**, 1247–1250.
13. K. W. Jung, Y. Kawahito, M. Takahashi and S. Katayama: 'Laser direct joining of carbon fiber reinforced plastic to zinc-coated steel', *Mater. Des.*, 2013, **47**, 179–188.
14. F. Balle, C. Wagner and D. Eifler: 'Ultrasonic spot welding of aluminium sheet/carbon fiber reinforced polymer joints', *Materialwiss. Werkstofftech.*, 2007, **38**, 934–938.
15. F. Balle, C. Wagner and D. Eifler: 'Ultrasonic metal welding of aluminium sheets to carbon fibre reinforced thermoplastic composites', *Adv. Eng. Mater.*, 2009, **11**, 35–39.
16. R. S. Mishra and Z. Y. Ma: 'Friction stir welding and processing', *Mater. Sci. Eng. R*, 2005, **R50**, 1–78.
17. F. C. Liu and Z. Y. Ma: 'Influence of tool dimension and welding parameters on microstructure and mechanical properties of friction-stir-welded 6061-T651 aluminum alloy', *Metall. Mater. Trans. A*, 2008, **39A**, 2378–2388.
18. J. Liao, N. Yamamoto and K. Nakata: 'Effect of dispersed intermetallic particles on microstructural evolution in the friction stir weld of a fine-grained magnesium alloy', *Metall. Mater. Trans. A*, 2009, **40A**, 2212–2219.
19. R. S. Lehrle, I. W. Parsons and M. Rollinson: 'Thermal degradation mechanisms of nylon 6 deduced from kinetic studies by pyrolysis-G.C.', *Polym. Degrad. Stab.*, 2000, **67**, 21–33.
20. S. H. Chowdhury, D. L. Chen, S. D. Bhole, X. Cao and P. Wanjara: 'Lap shear strength and fatigue life of friction stir spot welded AZ31 magnesium and 5754 aluminum alloys', *Mater. Sci. Eng. A*, 2012, **A556**, 500–509.
21. P. A. Colegrove and H. R. Shercliff: 'Development of Trivex friction stir welding tool. Part 1: two-dimensional flow modelling and experimental validation', *Sci. Technol. Weld. Join.*, 2004, **9**, 345–351.